

Research on Low-voltage Series Arc Fault Detection Method Based on Least Squares Support Vector Machine

Kai Yang, Rencheng Zhang*, Jianhong Yang, Yongzhi Chen and Shouhong Chen

College of Mechanical Engineering and Automation, Huaqiao University, Xiamen, 361021, China

Abstract: Arc fault is one of the important reasons of electrical fires. In virtue of cross talk, randomness and weakness of series arc faults in low-voltage circuits, very few of techniques have been well used to protect loads from series arc faults. Thus, a novel detection method based on support vector machine is developed in this paper. If series arc fault occurs, high frequency signal energy in circuit will increase a lot, and current cycle integrals are variable and erratic. However, high frequency signal energy will be influenced by cross talk in a nearby branch circuit. Besides, current cycle integrals will also vary while the working states of circuit changed. To better describe series arc faults, two characteristics include high frequency signal energy and current integral difference are extracted as support vectors. Based on these support vectors, least squares support vector machine is used to distinguish series arc faults from normal working states. The validity of the developed method is verified via an arc fault experimental platform set up. The results show that series arc faults are well detected based on the developed method.

Keywords: Arc fault detection, current integral, high frequency signal energy, least squares support vector machine.

1. INTRODUCTION

In the light of statistical data from fire services, arc faults, over currents, short circuits, and leakages are the main reasons of electrical fires, and over 90% of electrical fires are caused by them [1-3]. Leakage protectors and overcurrent breakers are used to protect electrical circuits from leakages and overcurrent circuits in the present, but they can't be used to prevent arc faults. There are three types of arc faults which contain earth arc fault, parallel arc fault and series arc fault. The characteristics of the former two are respectively similar to ground fault and over current. Hence, they are easy to be diagnosed [4]. However, fault characteristics of series arc faults are usually covered by load currents and background noise, making accurate recognition a difficulty of current research.

As a result of the randomness, weakness and cross talk of arc faults, there are some limitations in the methods which are based on arc light, arc sound wave, arc voltage and arc temperature appeared on stationary parts [5-9], and many arc models are usually too complex and inaccurate [10-13]. It is hard to put these methods to apply in facts while the locations of arc faults in circuits are uncertainty in most of time. Thus, in order to heighten the accuracy of the fault diagnosis in the process of arc fault detection, a large number of arc fault signals are collected to analyze general features. The features of high frequency signals and current integrals are extracted as support vectors to classify normal states and arc fault states. At last, a novel series arc fault detection method

which is based on least squares support vector machine (LSSVM) is researched in this paper.

2. EXPERIMENTAL PLATFORM ESTABLISHMENT AND DATA ACQUISITION

An arc fault experimental platform which is based on the low-voltage electric specifications is established as shown in Fig. (1). Standards include UL1699, IEC 62606: 2013 and JB/T11681-2013 are used as reference criterions to set up an experimental platform. Typical experimental loads are composed of six 50 W halogen lamps, a 0.75 kW electrical hand drill, two 40 W fluorescent lamps, a 0.35 kW computer, a 1.2 kW electric stove, a 1 kW dimming lamp, a 1.2 kW vacuum cleaner, 1.5/3.0 H.P. air conditioners and a 2.2 kW air compressor, etc. An arc generator consists of a stationary electrode and a moving electrode is used for simulation of arc fault in circuits. PXI data acquisition system and current transducers are used to acquire a large number of signals in circuits. And different kinds of loads' signals in arc faults and normal working states are used to analyze the universal characteristics.

3. ARC FAULT CHARACTERISTICS ANALYSIS AND EXTRACTION

3.1 Analysis of High Frequency Signal Energy

From a lot of arc fault experiments, high frequency signals are discovered as a reflection of the dynamic arc discharge process. They can be acquired by the high frequency transducer. During the initiation of arc extinguishing, many air molecules in the wire gap begin to be ionized, and the

*Address correspondence to this author at the College of Mechanical Engineering and Automation, Huaqiao University, Xiamen, 361021, China; Tel: +86 592 6162566; E-mail: phzzrc@hqu.edu.cn

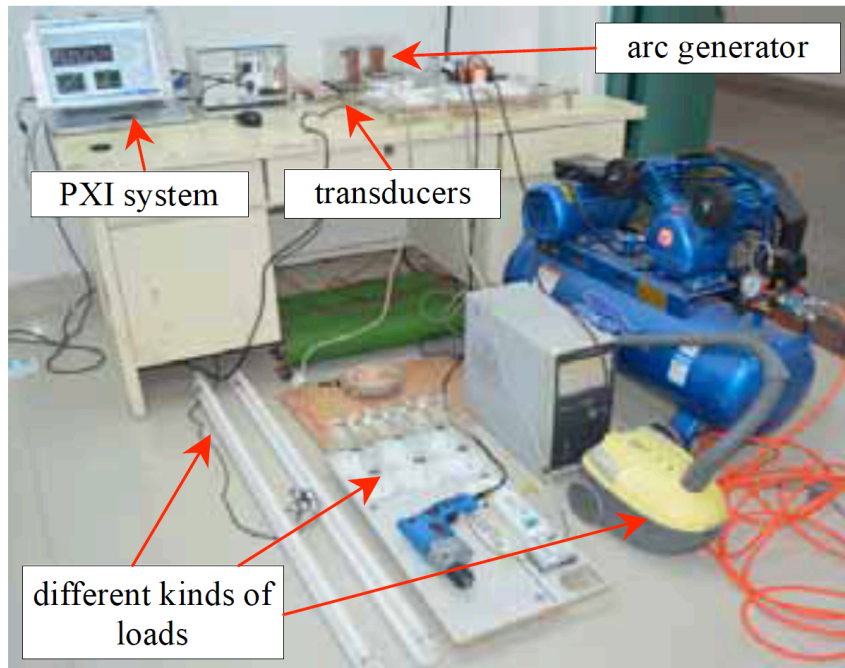


Fig. (1). Arc fault experimental platform.

motion of plasma is intensified further. According to electromagnetic theory, there are a great quantity of high frequency signals to be released at first. Then they will reduce gradually at the rest of current cycle. Therefore, cycles of high frequency signals will be produced when arc faults occur. However, these signals are uncertainty as a result of the unknown external conditions include the effects of electrode materials, surface states, oxide layers, adsorbed gases, arc currents, arc gaps of dielectric materials, and so on. Besides, the frequency spectrum of arc fault signal is chosen up to 50 MHz in order to facilitate characteristic analysis.

In order to find the common characteristics of arc fault, some typical load signals are selected to analysis. Arc fault signals are non-stationary, so their statistics, such as frequency spectrums, power spectrums and so on, are time-varying functions. To determine the amount of energy in a specific time and a frequency range, short time Fourier transform (STFT) is introduced to analysis arc fault signals. The high frequency signals and time-frequency diagrams of dimming lamp normal state and arc fault are shown in Fig. (2). As shown in Fig. (2a and b), there are some short pulses in the opening moments of SCR when the dimming lamp works in normal state or arc fault. And there are many high-frequency signals and short pulses during the arcing process when the dimming lamp works in arc fault. What's more, the high frequency signals with big amplitudes are densely distributed. From the frequency spectrum of normal state and arc fault that shown in Fig. (2c and d), the high frequency signals with 8~12 MHz are obvious when arc faults occur.

Another typical load is the vacuum cleaner, its high frequency signals and time-frequency diagrams of arc fault and normal state are shown in Fig. (3). When the vacuum cleaner works in normal state, there are some pulses to appear in the

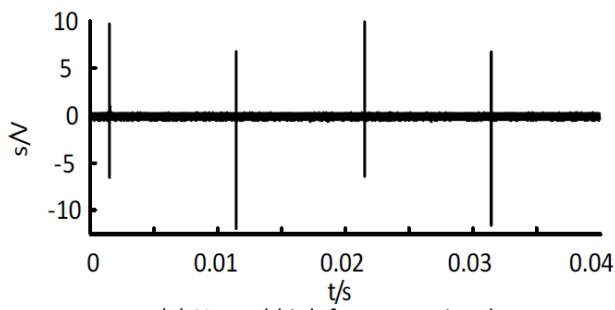
circuit because there is an electric brush motor in the vacuum cleaner as shown in Fig. (3a). Electrical discharge will happen and high frequency signals will be produced when the electric brush change the current phase. Fortunately, the high frequency signal amplitudes of vacuum cleaner arc fault are big and the signals are densely distributed as shown in Fig. (3b). The high frequency signals focus on 8~12 MHz of arc fault are more obvious than that of normal state as shown in Fig. (3c and d).

In summary, when series arc faults occur in circuits, there are many high frequency signals and their energy will increase immediately. The signal cycle energy $E(n)$ can be calculated by the formula listed as follows:

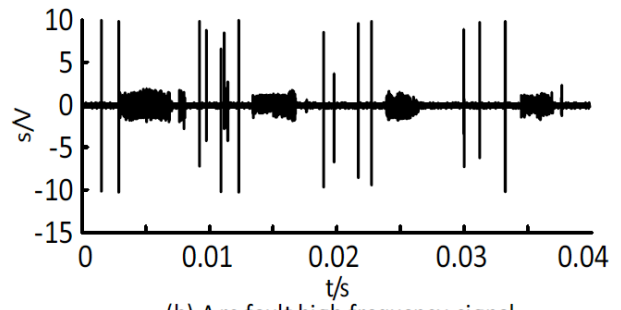
$$E(n) = \int_{(n-1)T}^{nT} s^2(t) dt \quad (n = 1, 2, \dots) \tag{1}$$

Here, T is an arc cycle which is 10 ms, $s(t)$ is the high frequency signal.

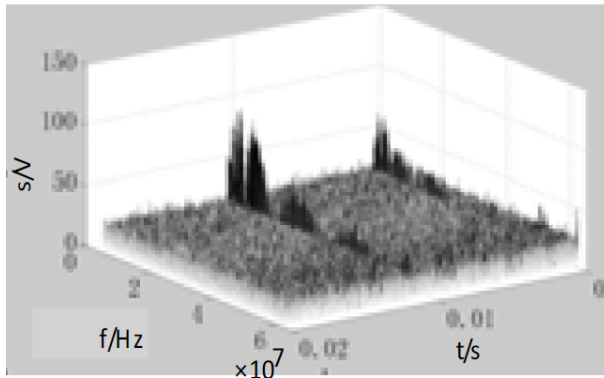
The high frequency signal energy of dimming lamp is shown in Fig. (2e and f), and that of vacuum cleaner is shown in Fig. (3e and f). From the energy distribution of them, it is not difficult to find that the high frequency signal energy of arc fault is more than that of normal state. However, the high frequency signal energy is different in different kinds of loads. It is hard to find a reasonable numerical value to classify the normal and the arc fault states in all loads just by a constant threshold. What's worse, the high frequency signals of arc fault in a circuit can be detected by a high frequency current transducer in a nearby branch circuit which is in normal state as a result of cross talk's influence. So it will cause misjudgment. To better distinguish arc faults from normal states, another characteristic might be added for judgment at the same time.



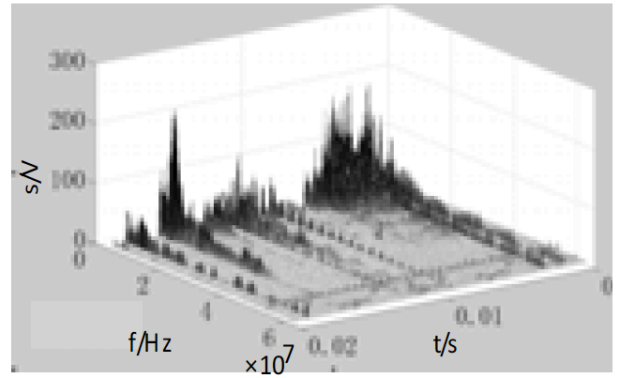
(a) Normal high frequency signal



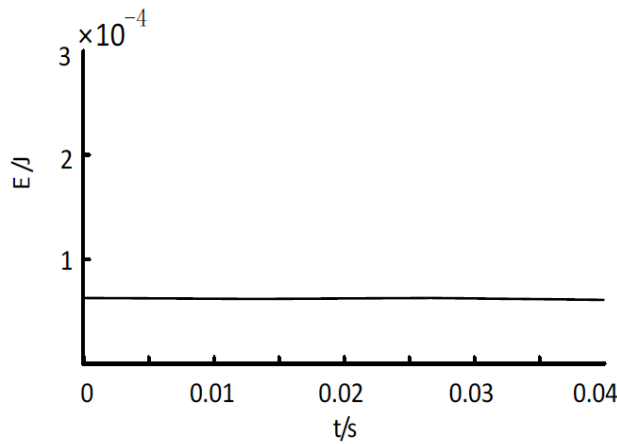
(b) Arc fault high frequency signal



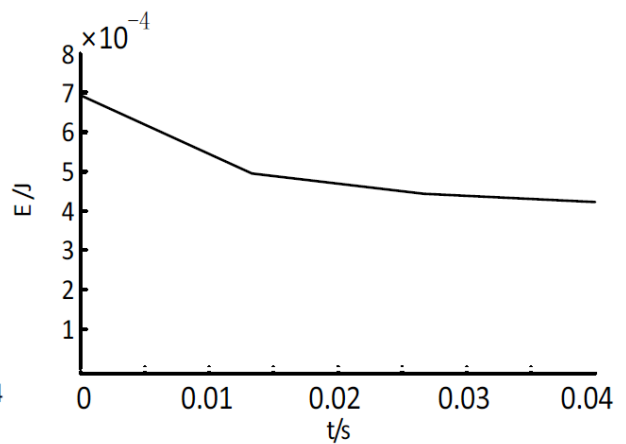
(c) Normal high frequency signal time-frequency diagram



(d) Arc fault high frequency signal time-frequency diagram

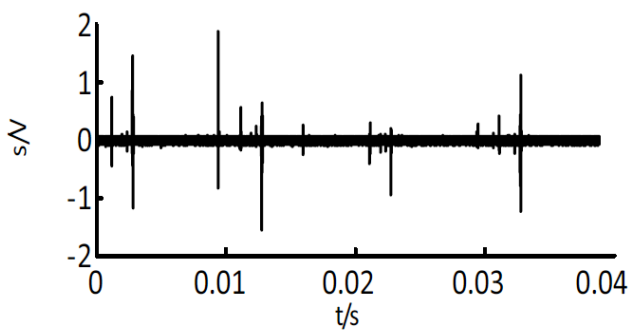


(e) Normal high frequency signal energy

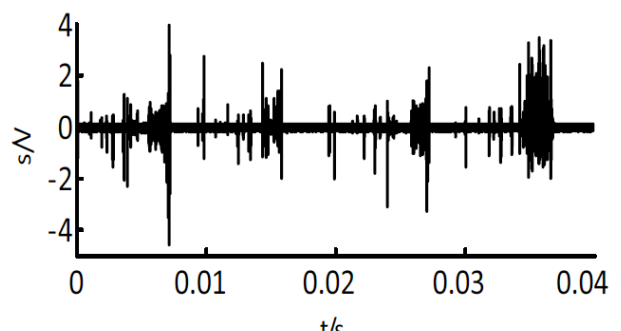


(f) Arc fault high frequency signal energy

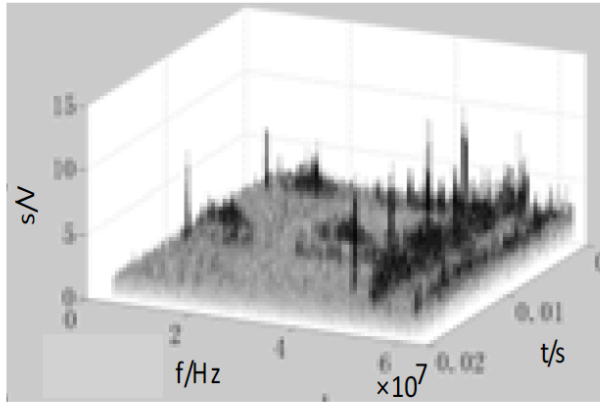
Fig. (2). Time-frequency analysis of dimming lamp's signals.



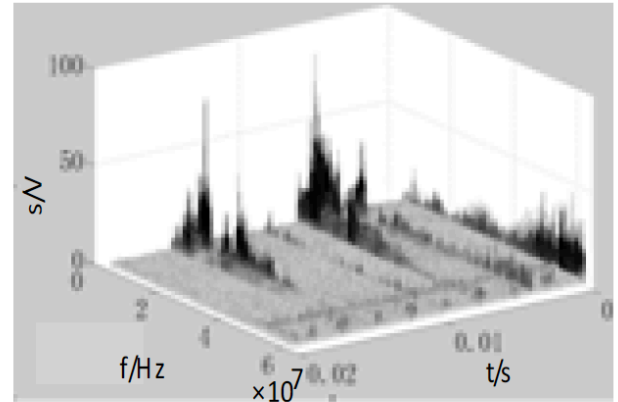
(a) Normal high frequency signal



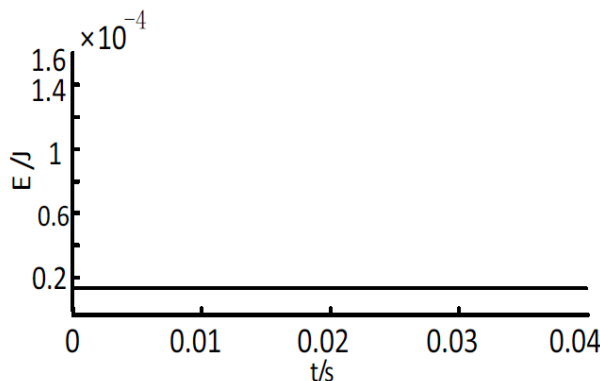
(b) Arc fault high frequency signal



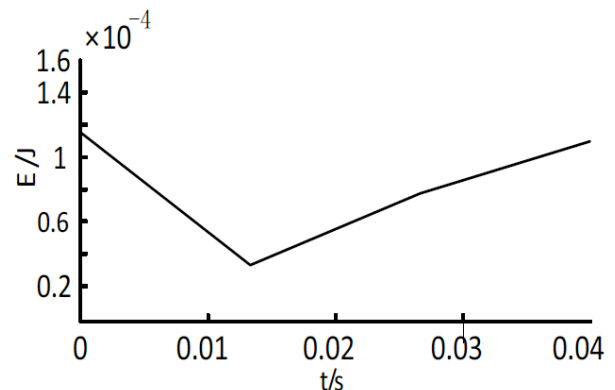
(c) Normal high frequency signal time-frequency diagram



(d) Arc fault high frequency signal time-frequency diagram



(e) Normal high frequency signal energy



(f) Arc fault high frequency signal energy

Fig. (3). Time-frequency analysis of vacuum cleaner’s signals.

3.2. Analysis of Current Integrals

Many kinds of working states’ typical load currents are shown in Figs. (4 and 5). The figures show that currents are relatively stable when loads are in normal states. But current periodicities will be lost, and current amplitudes will change evidently in an asymmetric manner when arc faults occur. What’s more, the current amplitudes will sometimes come to zero. Thus, whether an arc generated in the circuit or not may be discovered from the current integrals of cycles. The formula is listed as follows:

$$J(n) = \int_{(n-1)T}^{nT} c(t) dt \quad (n = 1, 2, \dots) \quad (2)$$

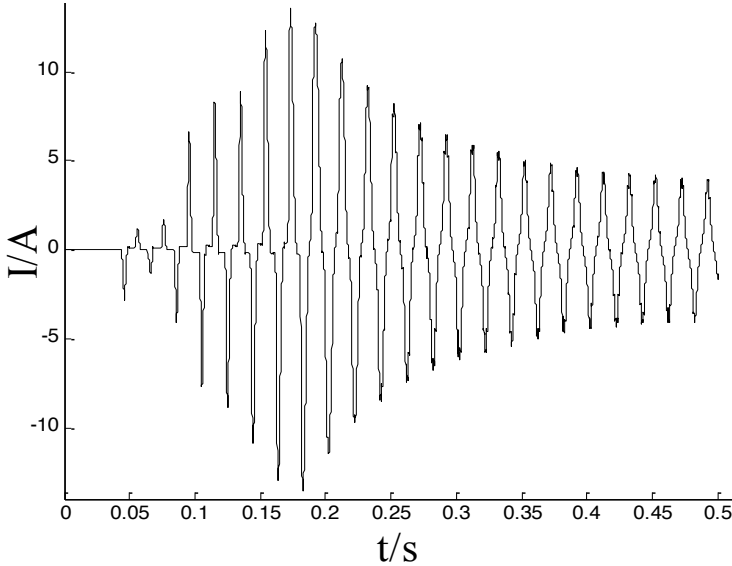
Here, T is an arc cycle which is 10 ms, $c(t)$ is the current of circuit.

When loads are in normal states, there are several working states such as plugging on and off, speed adjustment, load startup, and so on. And amplitude changes, shocks and other phenomena might be found in load currents. Some typical distorted currents caused by non-arc faults are shown in Fig. (4), the load arc fault currents are shown in Fig. (5). The current cycle integral difference can also be observed during

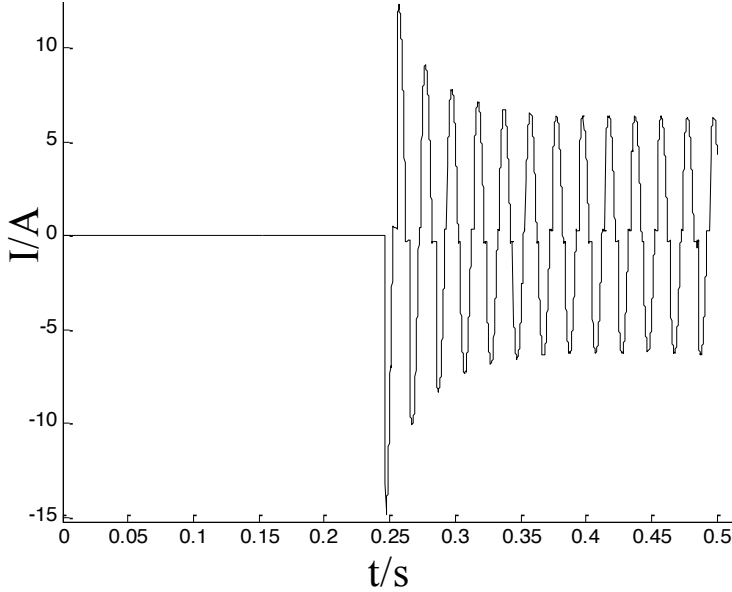
the normal working states. The halogen lamp currents of transient processes, such as start, adjustment and so on, will change as shown in Fig. (6a). The current cycle integrals change in a law and the integral variations are monotonic in a period of time as shown in Fig. (6b). Nevertheless, the amplitudes of current will change uncertainly and there are big fluctuations appeared in the current integrals when series arc fault occurs in circuit as shown in Fig. (7a and b).

The current and its integrals of vacuum cleaner in normal working state are shown in Fig. (8a and b). Though the current will change obviously when the cleaner speed is adjusted, the changes of current cycle integral are regular in a period of time. However, when series arc fault occurs in the vacuum cleaner as the current shown in Fig. (9), the amplitudes of current will fluctuate seriously, the wave of current will change obvious distortedly, and the current cycle integrals are erratic which are quite different from that of normal states.

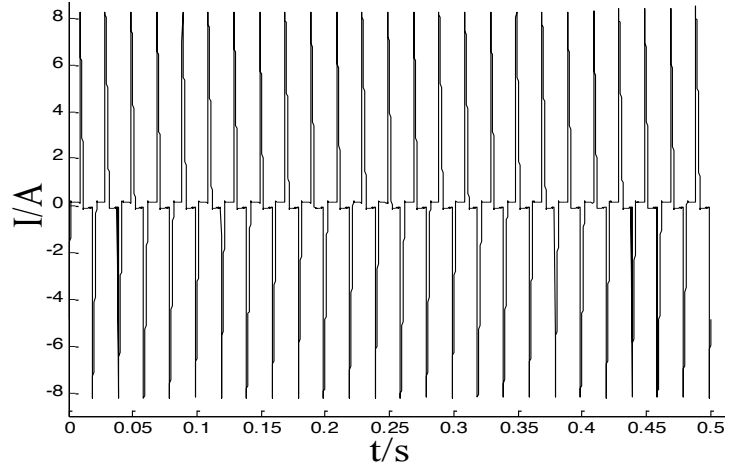
However, there are some limitations to detect arc faults just through current cycle integrals which will also change while the working states are adjusted. Therefore, the current integral variations may be used to further distinguish series



(a)



(b)



(c)

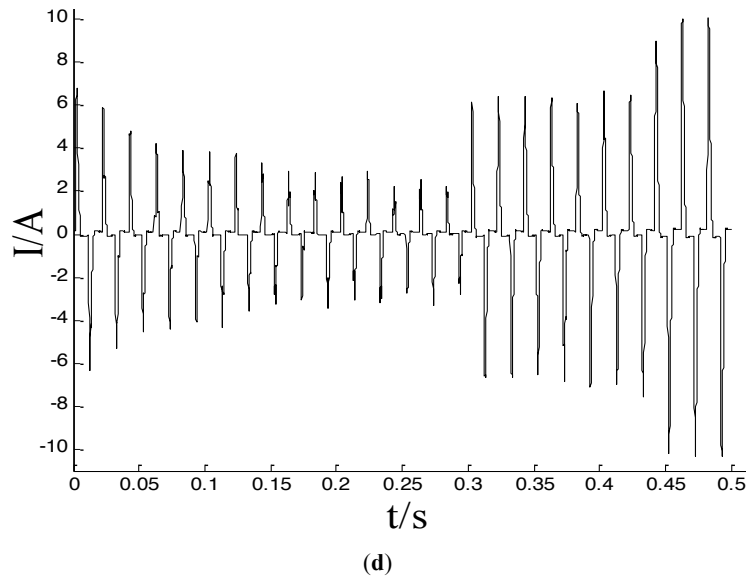
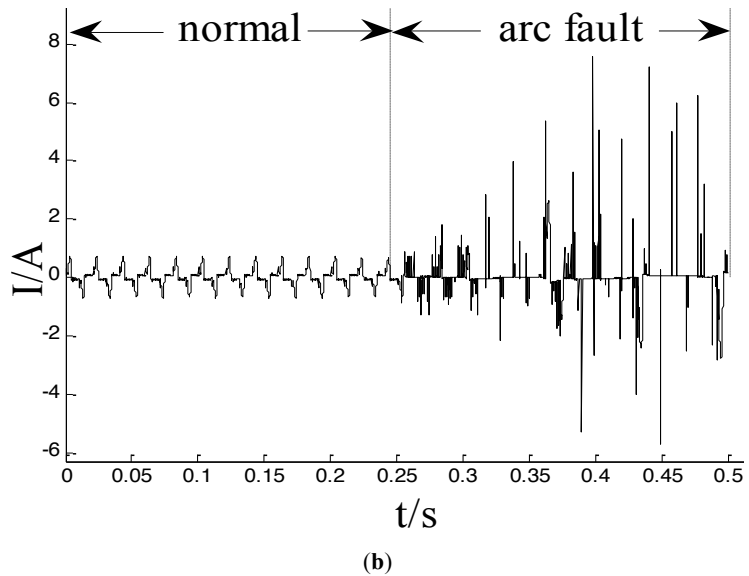
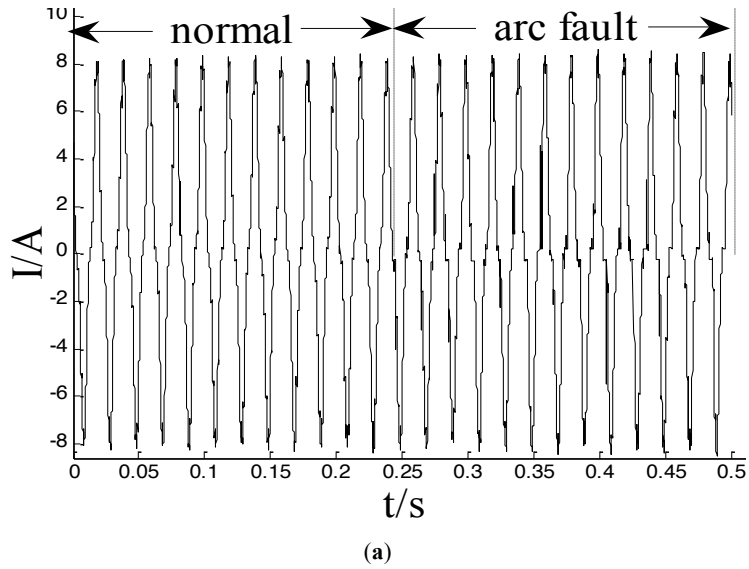


Fig. (4). Currents in non-arc faults: (a) start a hand drill, (b) plug a lamp, (c) dim a lamp, (d) adjust the vacuum cleaner speed.



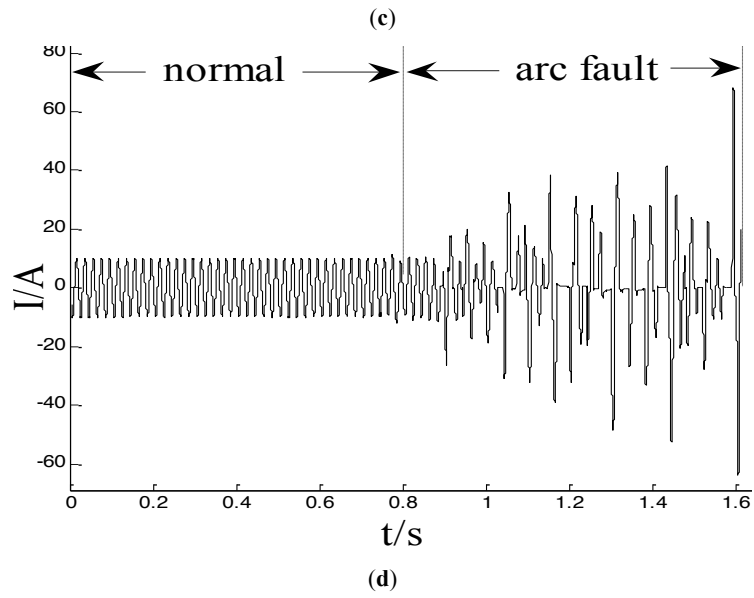
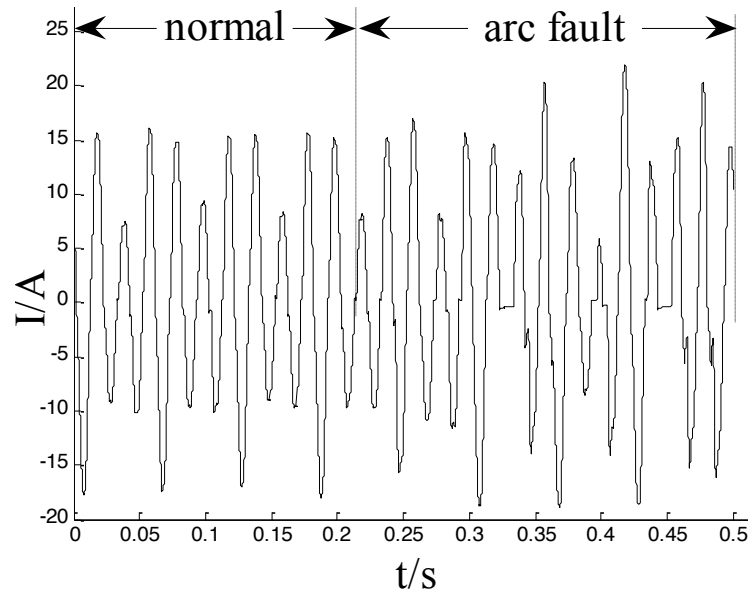
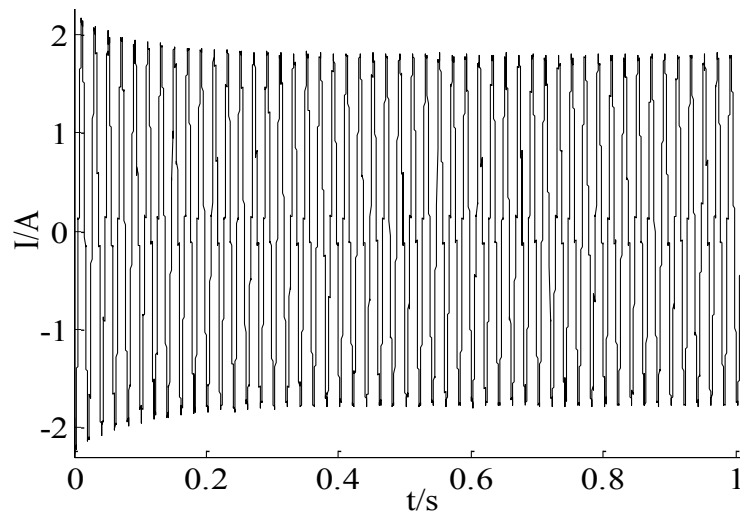
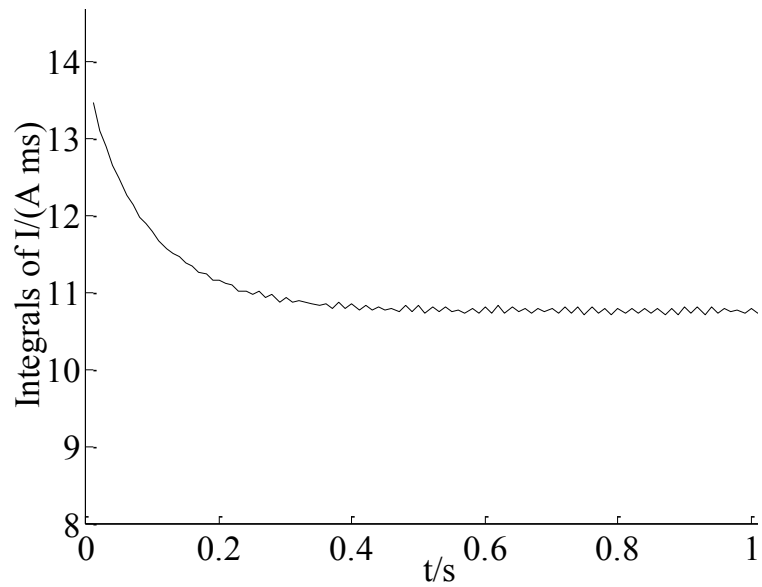
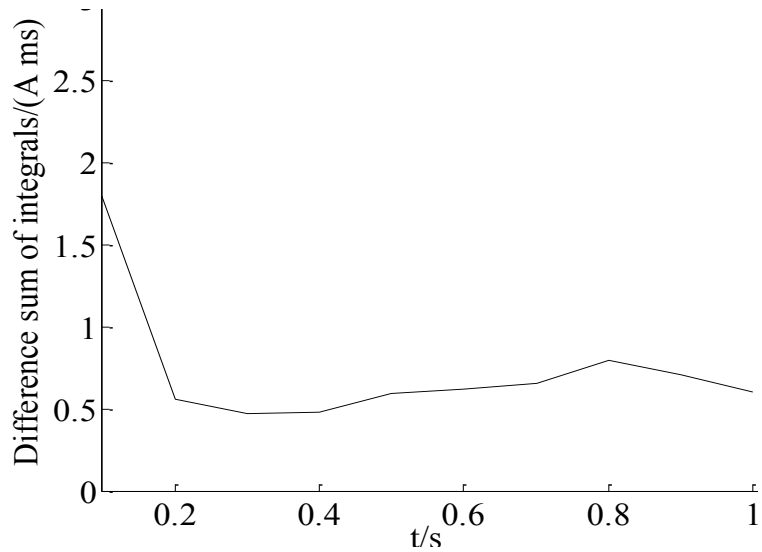


Fig. (5). Load currents: (a) electric stove, (b) computer, (c) air compressor, (d) air conditioner.



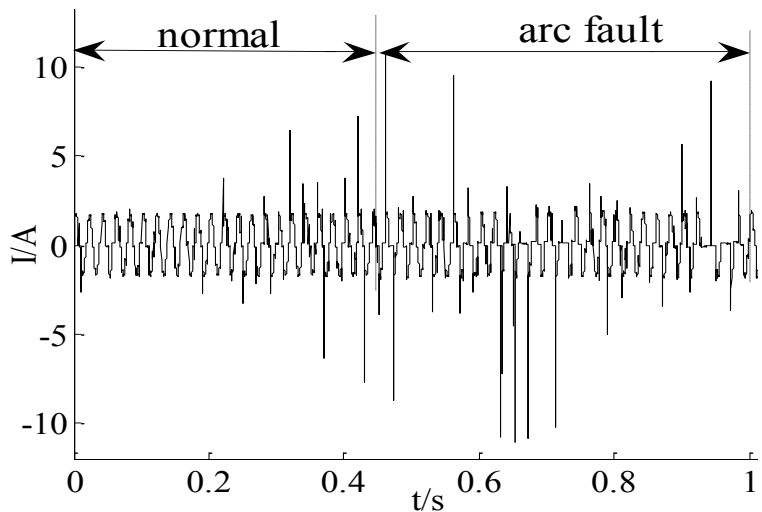


(b) Current cycle integrals

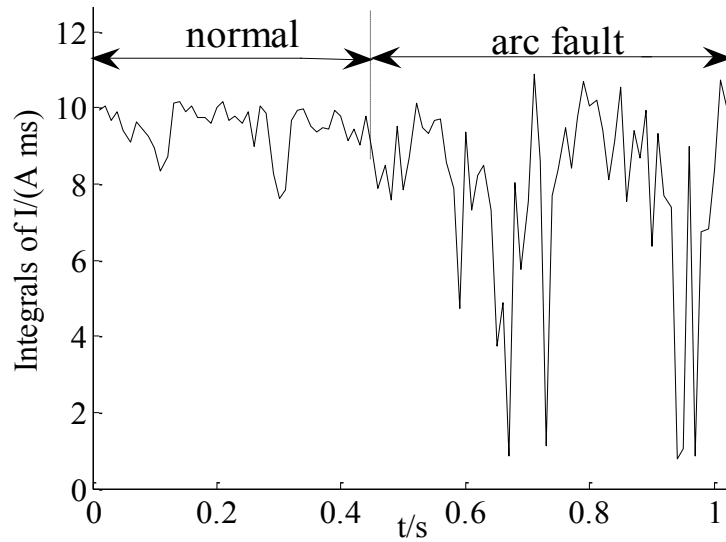


(c) Difference sum of integrals

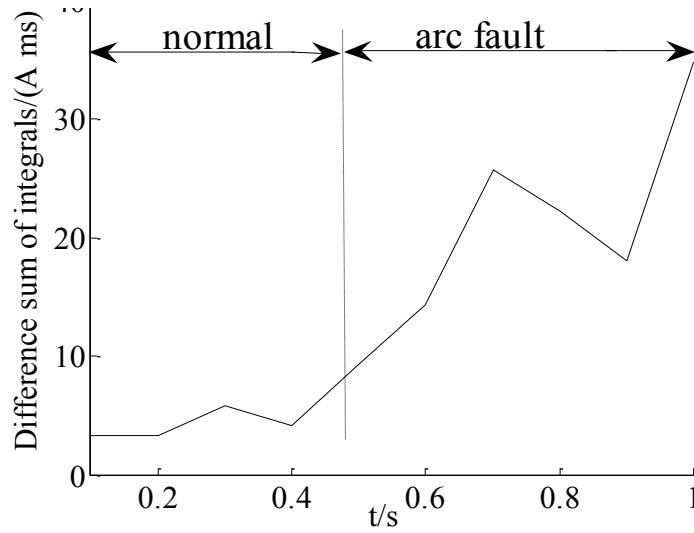
Fig. (6). Analysis starting current of halogen lamps.



(a) Current wave

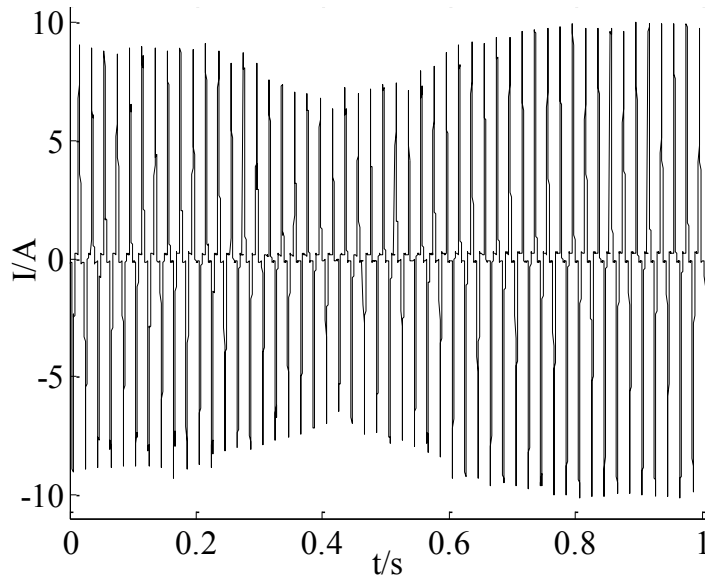


(b) Current cycle integrals

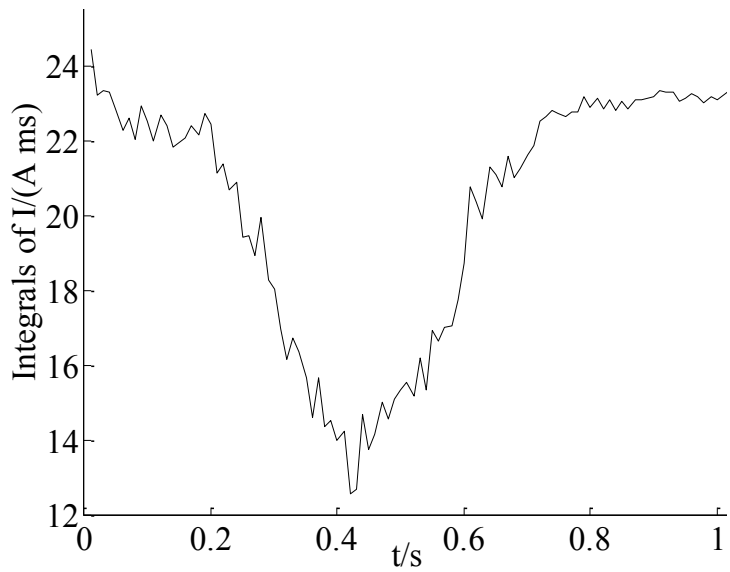


(c) Difference sum of integrals

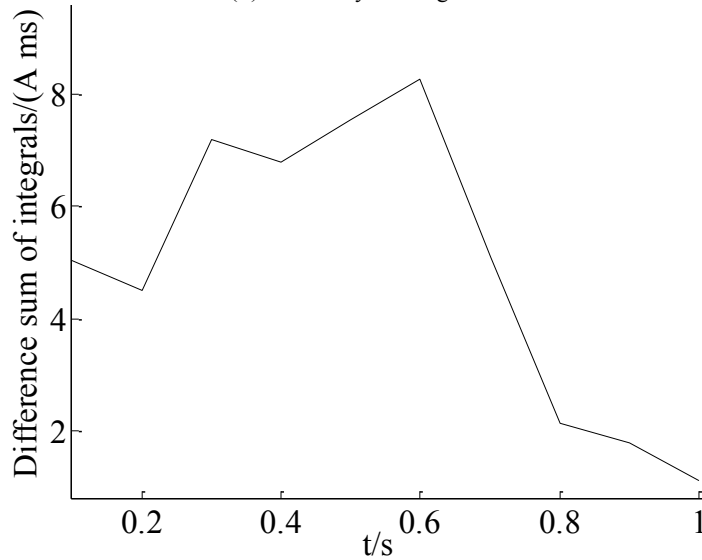
Fig. (7). Analysis arc fault current of halogen lamps.



(a) Current wave

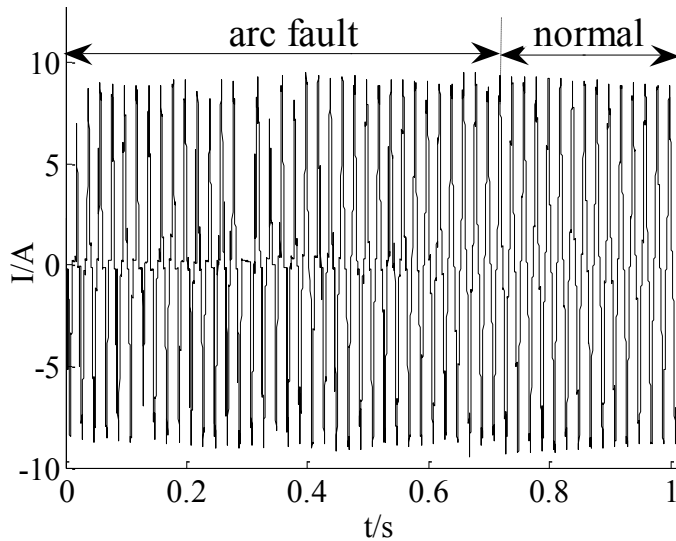


(b) Current cycle integrals

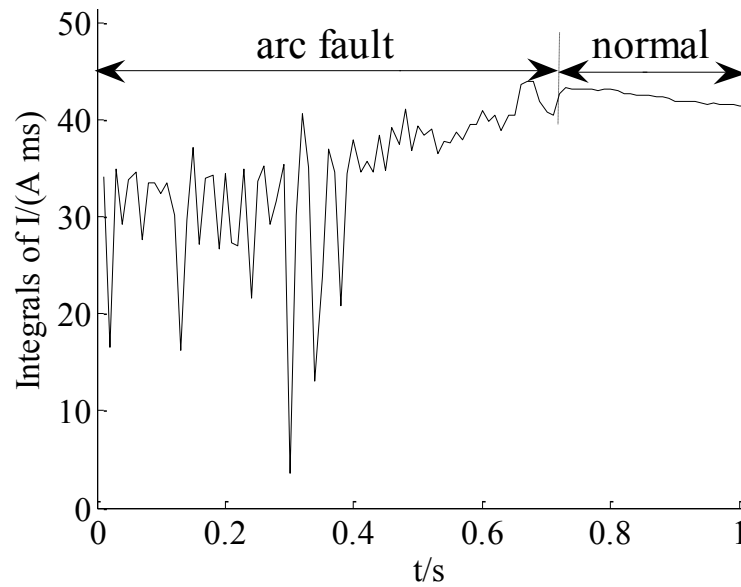


(c) Difference sum of integrals

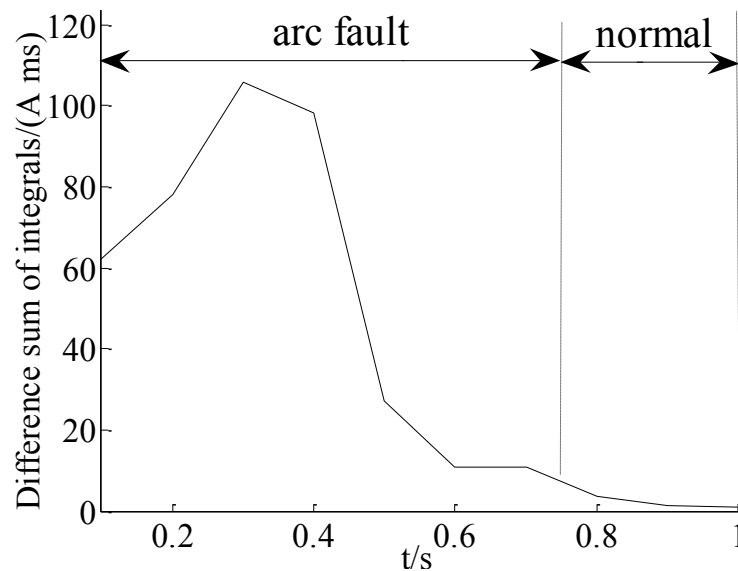
Fig. (8). Analysis speed adjustment current of the vacuum cleaner.



(a) Current wave



(b) Current cycle integrals



(c) Difference sum of integrals

Fig. (9). Analysis arc fault current of the vacuum cleaner.

arc faults from non-arc faults. In order to more accurately describe the variations, the difference sum of load's current integrals in a period of time is calculated by the formula (3):

$$D(n) = \sum_{n=1}^N (J(n+1) - J(n)) \quad (n=1, 2, \dots, N) \quad (3)$$

Here, $N = 10$, so the period of time is 100 ms.

The difference sum diagrams of halogen lamps and the vacuum cleaner are respectively shown in Fig. (6c), Fig. (7c), Fig. (8c) and Fig. (9c). From the analysis of a large number of loads' signals, it is not difficult to find that the classifying thresholds are different in different loads and working states through the difference sum of loads' current integrals. Take arc faults and speed adjustment states for example, the current integral difference sum of some halogen lamp arc faults is very closed to that of vacuum cleaner speed adjustment

states as shown in Figs. (7c and 8c). So it may cause misjudgment. According to all the analysis above, several characteristics should be chosen, and some intelligent classification algorithms [14, 15] would be introduced for the accurate identification of arc fault.

4. ARC FAULT IDENTIFICATION BASED ON LSSVM

When series arc fault occurs in circuit, high frequency signal energy of arc will increase a lot, and current integrals of cycles are variable and erratic. However, high frequency signal energy will be influenced by cross talk in a nearby branch circuit. Besides, current integrals of cycles will also vary while the working states of circuit change. And it is hard to find a reasonable constant threshold to classify the normal and the arc fault states in all loads. To better discrim-

inate arc fault states from normal states, two characteristics include high frequency signal energy and current integral difference are extracted. Based on these characteristics, support vector machine (SVM) is introduced to classify series arc faults and non-arc faults.

The SVM algorithm which is based on statistical learning theory has been successfully used to solve function estimation and classification problems [15]. The LSSVM algorithm which has been developed by Suykens and Vandewalle is a new deformation algorithm on the basis of the traditional SVM [16]. It can reduce computing complexity and guarantee the accuracy of the data classification at the same time. Two characteristics which are described by the vector $\mathbf{x}=[\mathbf{x}_1, \mathbf{x}_2]$ are listed as follows:

- 1) \mathbf{x}_1 , the high frequency signal energy of different kinds of loads.
- 2) \mathbf{x}_2 , the difference sum of load current integrals in a period of time.

The characteristic vector \mathbf{x} is mapped from the original space to the high dimensional feature space by non-linear transformation $f(\mathbf{x})$. Then, the optimal classification plane is found in the high dimensional feature space. According to the structural risk minimization principle, the constrained optimization problem corresponding to the original classification problem can be expressed as follows [17-19]:

$$\begin{cases} \min \left(\frac{1}{2} \mathbf{V}^T \mathbf{V} + \frac{C}{2} \sum_{i=1}^m \xi_i^2 \right) \\ \text{s.t. } y_i (\mathbf{V}^T f(\mathbf{x}_i) + b) = 1 - \xi_i \quad (i=1, \dots, m) \end{cases} \quad (4)$$

Here, \mathbf{V} is a weight vector. C is a penalty factor. m is the number of training samples. ξ_i is the relaxation coefficient of \mathbf{x}_i . b is a bias term. And the output result of classification is

$$y_i = \begin{cases} 1, & \text{if } \mathbf{x}_i \in \text{class 1} \\ -1, & \text{if } \mathbf{x}_i \in \text{class 2} \end{cases}$$

In order to solve the constrained optimization problem, lagrange multipliers α_i is introduced. So the formula (4) is transformed to the unconstrained objective function

$$L(\mathbf{V}, \delta, \alpha, b) = \frac{1}{2} \mathbf{V}^T \mathbf{V} + \frac{C}{2} \sum_{i=1}^m \xi_i^2 - \sum_{i=1}^m \alpha_i \{ y_i [\mathbf{V}^T f(\mathbf{x}_i) + b] - 1 + \xi_i \} \quad (5)$$

Here, $\alpha = (\alpha_1, \dots, \alpha_m)$, $\xi = (\xi_1, \dots, \xi_m)$.

According to the Karush- Kuhn-Tucker condition, let the derivative to \mathbf{V} , b , α_i , ξ_i of formula (5) equal to 0. Then, the equation can be expressed as

$$\begin{cases} y_i (\mathbf{V}^T f(\mathbf{x}_i) + b) - 1 + \xi_i = 0 \\ \mathbf{V} = \sum_{i=1}^m \alpha_i y_i f(\mathbf{x}_i) \\ \sum_{i=1}^m \alpha_i y_i = 0 \\ \alpha_i = C \xi_i \quad (i=1, \dots, m) \end{cases} \quad (6)$$

Furthermore, the equation (6) can be organized into a matrix form

$$\begin{pmatrix} \mathbf{\Omega} & \mathbf{y} \\ -\mathbf{y}^T & 0 \end{pmatrix} \begin{pmatrix} \alpha \\ b \end{pmatrix} = \begin{pmatrix} \mathbf{R} \\ 0 \end{pmatrix} \quad (7)$$

Here, $\mathbf{R} = (1, \dots, 1)^T$, $\mathbf{y} = (y_1, \dots, y_m)^T$, element in the positive definite matrix $\mathbf{\Omega}$ is

$$\Omega_{ij} = y_i y_j f^T(\mathbf{x}_i) f(\mathbf{x}_j) + \frac{\delta_{ij}}{C} = y_i y_j K(\mathbf{x}_i, \mathbf{x}_j) + \frac{\delta_{ij}}{C},$$

$$\delta_{ij} = \begin{cases} 1 & i = j \\ 0 & i \neq j \end{cases}. \text{ On the basis of Mercer condition,}$$

$K(\mathbf{x}_i, \mathbf{x}_j) = f^T(\mathbf{x}_i) f(\mathbf{x}_j)$ is defined as a kernel function.

According to the process of large amounts of arc fault data, radial basis function (RBF) is selected as the kernel function. And the model of arc fault classification is stable. The effect of classification is good.

Hence, the optimization problem of formula (4) can be solved by formula (7), α and b can be solved through least square method. The identification result of loads' states by LSSVM can be described as

$$y(\mathbf{x}) = \text{sgn} \left(\sum_{i=1}^m \alpha_i K(\mathbf{x}, \mathbf{x}_i) + b \right) \quad (8)$$

The main procedures of arc fault identification are listed as follows:

1) Select data set of LSSVM. The input is the characteristic vector \mathbf{x} include the high frequency signal energy \mathbf{x}_1 and the difference sum of current integrals \mathbf{x}_2 . And the output is the classification result \mathbf{y} , the status of output contains -1 and 1, '-1' represents the normal working state and '1' represents arc fault state.

2) Set up the recognizer sample Library (\mathbf{x}, \mathbf{y}) , here, \mathbf{x}_1 and \mathbf{x}_2 are characteristics, \mathbf{y} is output. From the experimental data of 9 kinds of loads in different working states, 300 sets of data are chosen to process. And 250 sets of them are treated as training samples; others are treated as testing samples. The recognizer sample library of arc fault is listed in Table 1.

3) Select kernel function parameters of RBF. In the light of cross validation method, reasonable kernel parameter σ^2 and penalty factor C will be found through the training sample set.

4) Identify arc fault. The testing samples are input into the arc fault recognizer. Then the identification results are compared with the real testing results. Finally, the generalization ability of recognizer is evaluated by error rate which can be calculated as

$$e = \frac{\sum_{i=1}^p |y_i^* - y_i|}{2p} \times 100\% \quad (9)$$

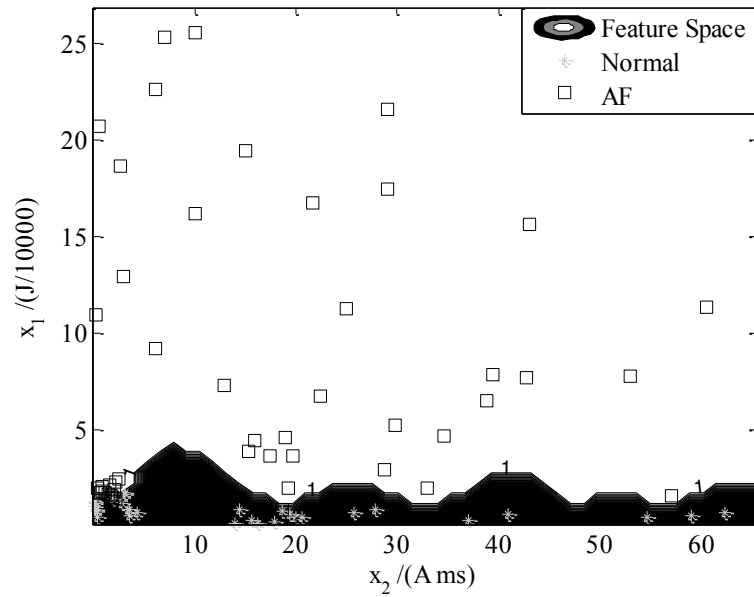


Fig. (10). Results of arc fault identification.

Table 1. The recognizer sample library.

Samples	1	2	...	299	300
x_1	1.72112	1.41022	...	0.68748	4.62154
x_2	0.64156	1.92081	...	40.10234	18.90978
y	1	-1		-1	1

Here, p is the number of testing samples. y_i^* is the real result of classification.

According to the main procedures of arc fault identification as listed above, the arc fault recognizer is set up. When the kernel parameter $\sigma^2=0.06$ and penalty factor $C=2.5$, the identification results are shown in Fig. (10). In that figure, “*” represents normal states of loads, and “□” represents arc faults of loads.

The testing samples can be identified through the characteristic space. If the testing sample appears at white area in Fig. (10), it means there is arc fault occurred; otherwise, there isn't arc fault in circuit. The identification results are the globally optimal solution in that RBF kernel function parameters, and the optimal classification plane of arc faults and normal states can be found in the high dimensional feature space.

In the experiments of the testing samples, the results show that the error rate of LSSVM is 4.0%. Hence, the arc fault identification rate is up to 96.0%. As a result of some situations with very weak arc fault signals are added into the testing samples, the high frequency signal energy and current integral difference of the arc faults are both very small, and they are very close to that of normal states. In that situation, the LSSVM recognizer fails to classify arc faults and normal states. Nevertheless, the dimension of characteristic vectors will be increased in the future algorithm improvement, and the identification accuracy will be improved.

CONCLUSION

In this paper, arc fault characteristics are extracted to realize the detection of series arc faults. The main conclusions are: 1) High frequency signal energy of arc will increase a lot when series arc fault occurs in circuit, but it will be influenced by cross talk in a nearby branch circuit. 2) Current integrals of cycles are variable and erratic while series arc fault occur in circuit, but they will also vary while the working states of circuit change. 3) Two characteristics contain high frequency signal energy and current integral difference are extracted at the same time to represent difference between the normal working states and arc fault states. 4) Based on these characteristics, LSSVM is successfully used to distinguish arc faults from normal working states, and the method is verified through the experimental platform. The arc fault detection rate is up to 96.0%. What's more, the developed method has a good ability of generalization.

CONFLICT OF INTEREST

The authors confirm that this article content has no conflict of interest.

ACKNOWLEDGEMENTS

This work was supported by the Fujian Natural Science Foundation (2012JH01214), the Fujian Industry-University Cooperation Science & Technology Major Project

(2012H6013), the Xiamen Science & technology project (3502Z20143043) and the Quanzhou Science & technology project of China (2014Z114).

REFERENCES

- [1] Fire Department of Ministry of Public Security, *2012 China Fire Services*, China Personnel Publishing House, Beijing, 2012.
- [2] G. Si, "Analysis on China's electrical fire situation and feature from 2008 to 2012", *Fire Science and Technology*, vol. 33, no. 5, pp. 569-572, 2014.
- [3] C. N. Vadoli, "Lessons learned from electrical circuit analysis in support of a fire probabilistic risk assessment", In: *International Topical Meeting on Probabilistic Safety Assessment and Analysis*, 2011, pp. 711-720.
- [4] G. D. Gregory, K. Wong, and R. Dvorak, "More about arc-fault circuit interrupters", *IEEE Transaction on Industry Applications*, vol. 40, no. 4, pp. 1006-1011, 2004.
- [5] J. H. Yang, R. C. Zhang, and H. Y. Fang, "Early detecting of fault arcs using Lyapunov exponents", *Advanced Technology of Electrical Engineering and Energy*, vol. 27, no. 2, pp. 56-58, 2008.
- [6] R. C. Zhang, J. H. Yang, and J. H. Du, "Study on in-process detection and diagnosis of faults arc based on early sounds signature and intermittent chaos", *Key Engineering Materials*, vol. 381-382, pp. 611-614, 2008.
- [7] J. K. Charles, "Electromagnetic radiation behavior of low-voltage arcing fault", *IEEE Transactions on Power Delivery*, vol. 24, no. 1, pp. 416-423, 2009.
- [8] R. C. Zhang, and J. H. Du, "Fuzzy clustering algorithm of early fire based on process characteristic", *Key Engineering Materials*, vol. 437, pp. 339-343, 2010.
- [9] M. Rabla, P. Schweitzer, and E. Tisserand, "Method to design arc fault detection algorithm using FPGA", *IEEE 57th Holm Conference on Electrical Contacts*, 2011, pp. 138-142.
- [10] T. Gammon, and J. Matthews, "Arcing-fault models for low-voltage power systems", In: *IEEE Industrial and Commercial Power Systems Technical Conference*, 2000, pp. 119-126.
- [11] H. R. Wu, X. H. Li, D. Stade, and H. Schau, "Arc fault model for low voltage AC systems", *IEEE Transactions on Power Delivery*, vol. 20, no. 2, pp. 1204-1205, 2005.
- [12] J. Lezama, P. Schweitzer, S. Weber, E. Tisserand, and P. Joyeux, "Modeling of a domestic electrical installation to arc fault detection", In: *58th IEEE Holm Conference on Electrical Contacts*, 2012, pp. 1-7.
- [13] G. Parise, L. Martirano, and M. Laurini, "Simplified arc-fault model: The reduction factor of the arc current", *IEEE Transactions on Industry Applications*, vol. 49, no. 4, pp. 1703-1710, 2013.
- [14] D. J. Yao, J. Yang, and X. J. Zhan, "An improved random forest algorithm for class-imbalanced data classification and its application in PAD risk factors analysis", *The Open Electrical & Electronic Engineering Journal*, vol. 7S1, pp. 62-70, 2013.
- [15] M. Pontil, and A. Verri, "Properties of support vector machines", *Neural Computation*, vol. 10, no. 4, pp. 955-974, 1998.
- [16] J. A. K. Suykens, and J. Vandewalle, "Least squares support vector machine classifiers," *Neural Processing Letters*, vol. 9, no. 3, pp. 293-300, 1999.
- [17] J. Deng, Y. Xiao, Y. P. Hao, L. C. Li, Y. M. Zhao, and J. G. Zhang, "Compound electric field prediction method for the UHVDC transmission lines based on fuzzy clustering and least squares support vector machine," *High Voltage Engineering*, vol. 39, no. 12, pp. 2987-2993, 2013.
- [18] X. W. Yang, L. J. Tan, and L. F. He, "A robust least squares support vector machine for regression and classification with noise," *Neurocomputing*, vol. 140, pp. 41-52, 2014.
- [19] Q. Cheng, J. Tezcan, and J. Cheng, "Confidence and prediction intervals for semiparametric mixed-effect least squares support vector machine," *Pattern Recognition Letters*, vol. 40, no. 1, pp. 88-95, 2014.

Received: June 09, 2015

Revised: June 22, 2015

Accepted: September 24, 2015

© Yang *et al.*; Licensee Bentham Open.

This is an open access article licensed under the terms of the Creative Commons Attribution Non-Commercial License (<http://creativecommons.org/licenses/by-nc/3.0/>) which permits unrestricted, non-commercial use, distribution and reproduction in any medium, provided the work is properly cited.